JOURNAL OF APPLIED ELECTROCHEMISTRY **28** (1998) 305–310

Development of a 100 W rechargeable bipolar zinc/oxygen battery*

S. MÜLLER, O. HAAS

Paul Scherrer Institute, CH-5232 Villigen PSI, Switzerland

C. SCHLATTER, Ch. COMNINELLIS

Swiss Federal Institute of Technology, CH-1015 Lausanne, Switzerland

Received 18 November 1996

A bipolar filter press-type electrically rechargeable Zn/O_2 battery has been developed. Reticulated copper foam served as substrate for the zinc deposit on the anodic side, and $La_{0.6}Ca_{0.4}CoO_3$-catalysed bifunctional oxygen electrodes were used on the cathodic side of the cells. The 100 cm^2 unit cell had an open circuit voltage of 1.4 V (O_2) in moderately alkaline electrolyte. The open circuit voltage and the peak power measured for a stack containing seven cells were ~10 V and ~90 W, respectively. The current–potential behaviour was determined as a function of the number of bipolar cells, and the maximum discharge capacity was determined at different discharge rates.

Keywords: *bipolar zinc/oxygen battery*, *zinc plated copper foam*, *bifunctional oxygen electrode*

List of symbols

A_s	specific surface area of the foam (m^{-1})
A_p	surface area of the Cu plate (m^2)
c	concentration (mol m^{-3})
D	diffusion coefficient ($m^2\,s^{-1}$)
d_h	equivalent hydraulic diameter, $d_h = 2\,\varepsilon lh(l+h)^{-1}$ (m)
F	Faraday constant, $F = 96\,484$ C mol^{-1}
h	electrode thickness (m)
l_f	peak current (Cu foam electrode) (A)
l_{lim}	limiting diffusion current (A)
l_p	peak current (Cu plate electrode) (A)
k_a	mass transfer coefficient (m s^{-1})
l	electrode width (m)
V	volume of the foam electrode (m^3)
v	scan rate (V s^{-1})
v_{el}	superficial electrolyte velocity (m s^{-1})
z	number of electrons
Re	Reynolds number, $Re = v_{el}d_h v^{-1}$
Sc	Schmidt number, $Sc = vD^{-1}$
Sh	Sherwood number, $Sh = k_a L_c D^{-1}$

Greek symbols

χ_{sol}	electrolyte conductivity ($\Omega^{-1}\,m^{-1}$)
ε	porosity
η	overpotential (V)
ρ	density ($kg\,m^{-3}$)
v	kinematic viscosity ($m^2\,s^{-1}$)

Physical properties of the electrolyte at 25 °C

Viscosity $= 5.35 \times 10^{-3}$ kg m^{-1} s^{-1}
Density $= 1450$ kg m^{-3}
Diffusion coefficient of zincate $= 6 \times 10^{-10}$ $m^2\,s^{-1}$
Conductivity $= 40\,\Omega^{-1}\,m^{-1}$
$c([Zn(OH)_4]^{2-})$ 180 mol m^{-3} for the first charging process
$Sc = 6149$

1. Introduction

A rechargeable battery providing both high specific energy and high specific power would be an attractive power source candidate for many applications. The Zn/air battery system has high energy density, good environmental compatibility, low cost of active materials and wide operating temperature range. However, major limitations of secondary Zn/air batteries have been their low specific power and low cyclability. Problems due to corrosion of the bifunctional oxygen electrode during charging of the battery and due to unfavourable changes in the Zn morphology on cycling have been reported [1, 2]. Nevertheless, a promising service life of 3000 h has been measured for perovskite-catalysed bifunctional oxygen electrodes cycled in monopolar Zn/oxygen cells with moderately alkaline electrolyte [3, 4].

The specific power of the battery can be considerably improved by enhancing the kinetics at the air electrode, the OH^- transport in the porous zinc electrode and by designing a compact cell showing less ohmic resistance.

Here we present results obtained with highly porous zinc electrodes and $La_{0.6}Ca_{0.4}CoO_3$-catalysed bifunctional O_2-electrodes in a bipolar configuration.

*This paper was presented at the Fourth European Symposium on Electrochemical Engineering, Prague, 28–30 August 1996.

In the bipolar system all cells are internally connected in series and the output is high voltage/low current, which is desirable for electric vehicle (EV) applications. Advantages of the bipolar over the monopolar system are the absence of external electrical connections to individual electrodes and cell-to-cell current flow through the whole area of the electrode. In principle, the conductivity requirement for the electrodes is less severe, and less expensive battery construction should be possible for the bipolar system.

Flow-through porous electrodes can be used for many applications such as fuel cells, redox energy storage systems, and chemical reactors or in primary and secondary batteries [5, 6]. The performance of some primary and secondary batteries may be enhanced by a fresh supply of electrolyte [7]. However, for bipolar flow-through systems, problems due to energy loss caused by leakage currents flowing along the common manifold have been reported [8]. Thus, for a flow-through bipolar Al/O_2 module, the shunt current problem was avoided by using separate electrolyte circuits [9]. Recently, Cooper *et al.* reported the development of a refuelable zinc/air module consisting ot twelve bipolar cells with an internal flow system. The module is refueled by entrainment of 0.5 mm Zn-particles in rapidly flowing electrolyte. Refueling would be done at a company's EV home base [10]. However, additional weight caused by the auxiliary system, e.g. peristaltic pump and separate electrolyte reservoirs, can considerably decrease the specific energy and power of the system.

In contrast to the mechanically rechargeable metal/air battery systems described above, we developed a hybrid system offering maintenance-free electrical recharging of the battery combined with regeneration of the system at periodic service intervals. While stationary, moderately alkaline electrolyte (chemically saturated with ZnO) was used for the electrically rechargeable operating mode, for the regeneration process of the battery highly alkaline electrolyte $+ 0.18$ M Zn^{2+} was pumped through the porous zinc electrode. Consequently, during cycling of the battery in moderately alkaline electrolyte, insoluble ZnO is formed in the porous electrode during discharge which can be reduced to metallic zinc during the following charging process. Because of Zn redistribution in the foam after a certain number of cycles, all Zn must then be stripped from the foam and new, well distributed metallic zinc built into the substrate by performing the regeneration process.

2. Experimental details

2.1. *Homogeneous formation of metallic zinc in porous Cu foam electrodes*

To form zinc homogeneously in the foam electrode during the first charge, the flow-by porous electrode configuration was applied. This configuration has the advantage that the flow of current is perpendicular to the fluid flow. Thus, the electrodes can be made thin to minimize the ohmic potential drop in the electrodes, and they can be made long in the flow direction to achieve high conversion. During the first charging of the cell, zinc was deposited from flowing 45 wt % KOH containing 0.18 M Zn^{2+}. An initial capacity of 8 A h was developed on the 100 cm^2 electrode. The influence of the electrolyte flow rate on the zinc distribution was studied for two foam materials (MN020, MN045, Sorapec(F)) differing in their specific surface area. The maximum thickness (h_{max}) of the porous Cu foam which still guarantees a homogeneous zinc deposition at the limiting diffusion current (l_{lim}) can be calculated according to Equation 1 [11]:

$$h_{max} = \sqrt{\left(\frac{2(\eta_2 - \eta_1)\chi_{sol}\varepsilon}{A_s k_a z F c}\right)} \quad (1)$$

The mass transfer coefficient (k_a) between the liquid and the electrode, as well as the specific surface area (A_s) of the two foam materials, were experimentally determined using the reduction of ferricyanide ions.

The specific surface area (A_s) of the metallic foams was determined by cyclic voltammetry. The peak current at different scan rates was measured for a copper plate (roughness factor 1) and for the foam materials. From the slope of the l_p against $v^{0.5}$ curves, A_s was calculated according to Equation 2:

$$A_s = \left(\frac{dI_f}{dv^{0.5}} \Big/ \frac{dI_p}{dv^{0.5}}\right)\frac{A_p}{V} \quad (2)$$

The mass transfer coefficient was measured at the limiting diffusion current for different electrolyte flow rates (Reynolds numbers, *Re*). The measurements of reactant concentration at the exit of the flow-through cell showed that the difference relative to the feed concentration was of the order of 5%. Under these experimental conditions, k_a follows Equation 3. To express the correlation between the mass transfer coefficient and the Reynolds number, the dimensionless expression (Equation 4) was used:

$$k_a = \frac{I_{lim}}{zFA_s Vc} \quad (3)$$

$$Sh = a\,Re^{\alpha}Sc^{0.33} \quad (4)$$

2.2. *Test conditions for the single cell and the Zn/oxygen module*

The battery was built in the configuration of a filter press. The components of a single cell and of the bipolar stack are depicted in Fig. 1. The main components of the bipolar cell were the zinc-plated reticulated copper foam anode (1 and 5), the $La_{0.6}Ca_{0.4}CoO_3$-catalysed bifunctional oxygen diffusion electrode (4), the PVC frames (2) for sealing the cells, and the cathode supports needed to constitute the zinc/oxygen cells in the bipolar arrangement (1 and 5). After the first charge (8 A h for the 100 cm^2 zinc electrode), the electrolyte was replaced by a 20 wt %

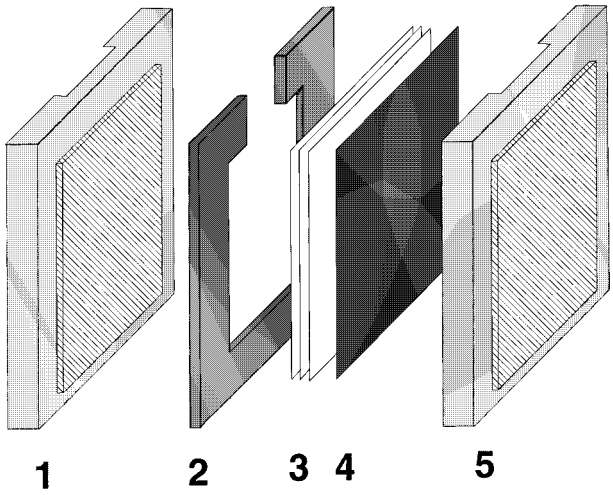

Fig. 1. Exploded view of the stack components: (1) bipolar element, (2) PVC frame, (3) separator, (4) bifunctional O_2-electrode, (5) bipolar element. Geometric surface area: 100 cm^2.

KOH solution presaturated with ZnO. Cycle life tests as well as current-potential measurements were carried out with stationary moderately alkaline electrolyte in which the following two consecutive reactions take place at the zinc electrode:

$$Zn + 4\,OH^- = Zn(OH)_4^{2-} + 2e^- \quad (5)$$

$$Zn(OH)_4^{2-} = ZnO + 2\,OH^- + H_2O \quad (6)$$

The electrochemical reaction (Equation 5) is followed by a dissolution-precipitation reaction (Equation 6). Cycling was performed at 10 mA cm^{-2} charging and 20 mA cm^{-2} discharging currents. The cycled capacity was 5 A h for the 100 cm^2 zinc electrode. At high discharge currents the Zn utilization is strongly influenced by OH^- transport into the reticulated foam electrode. To measure the recoverable capacity of the zinc-foam electrode at high discharge rates, galvanostatic discharge curves were measured for a single cell, as well as for a bipolar module with seven cells.

The current–potential curves were measured galvanostatically. For each chosen current the potential of the battery was measured after a cell operating time of 30 s. The power of the stack was calculated from measured current–voltage curves.

3. Results

3.1. *Characterization of the Cu foam electrodes*

In Fig. 2 the peak currents l_p extracted from the cyclic voltammograms measured with the electrochemical couple $Fe(CN)_6^{3-}/Fe(CN)_6^{4-}$ ($C(Fe^{2+}) = 2.5 \times 10^{-2}$ M and $C(Fe^{3+}) = 2.5 \times 10^{-3}$ M) at a planar Cu electrode ($A = 7\,cm^2$) and at the two foam electrodes MN020 and MN045 of 1.86 cm^3 are plotted against $v^{0.5}$. The corresponding specific surface areas of the reticulated electrodes calculated using Equation 2 are presented in Table 1.

The hydrodynamic conditions within the three-dimensional electrodes MN020 and MN045 at different electrolyte flow rates have been determined by measuring the mass transfer limited currents for the reduction of ferricyanide in 1 M KOH. In order to estimate a and α the logarithm of the Sherwood number was plotted against the logarithm of the Reynolds number as depicted in Fig. 3.

The values of the coefficients in the correlations expressed as Sh against Re are reported in Table 1 ($Sc = 1320$ [5]). The values of α are of the same order of magnitude as those given by Montillet *et al.* for metallic nickel foams in filter-press type cells [13]. The dimensionless relation was finally used for calculating the maximum thickness of the foam electrodes which still guarantees a homogeneous current distribution under limiting diffusion current conditions. For formation of the zinc deposits, the 45 wt% KOH solution was pumped with a flow rate of 6.0 ml s^{-1} through the porous foam electrodes. The corre-

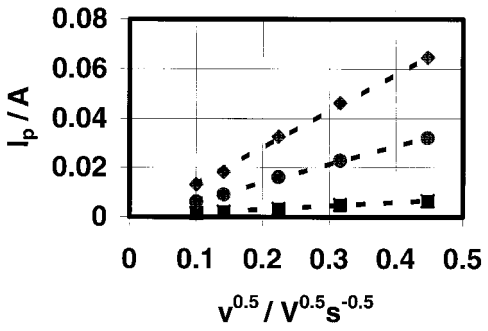

Fig. 2. Peak current against the root of the scan rate for the porous electrodes (●) MN020 and (◆) MN045 ($V = 1.86\,cm^3$) compared to a (■) planar Cu electrode ($A_{Cu} = 7\,cm^2$).

Table 1. Active and specific surface areas for 1 m^2 electrodes as well as fitted coefficients of the dimensionless expression (Equation 4) for the two foam materials and a planar electrode [12]

Cu foam electrodes	*Active surface area, A* /m^2	*Specific surface area, A_s* /m^{-1}	$Sh = a\,Re^{\alpha}Sc^{0.33}$
MN020 ($h = 5$ mm)	9.41	1882	$a = 0.726$ $\alpha = 0.527$
MN045 ($h = 2$ mm)	7.67	3836	$a = 0.574$ $\alpha = 0.437$
Planar electrode [12]	1	–	$a = 0.22$ $\alpha = 0.71$

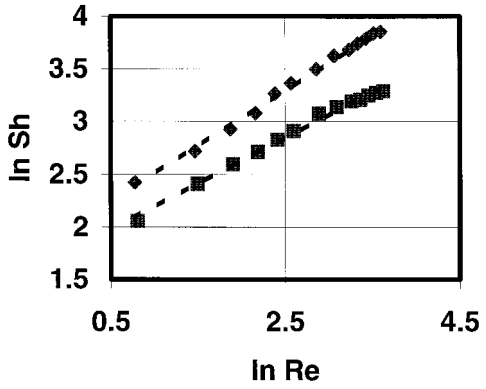

Fig. 3. Logarithm of Sherwood against logarithm of Reynolds determined for the porous electrodes (◆) MN020 and (■) MN045 in a flow-by configuration.

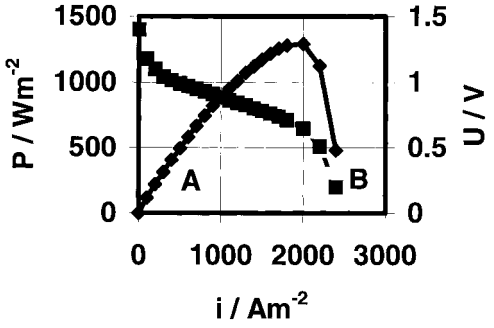

Fig. 4. Polarization curve for one cell using a 0.01 m^2 MN045 zinc foam electrode. Power density (A) and voltage of the cell (B) as functions of the current density.

sponding superficial electrolyte velocity and the *Re* number as well as *Sh* and k_a are listed in Table 2. Maximum thicknesses of ~ 7 mm and ~ 4 mm were calculated using Equation 1 for MN020 and MN045, respectively. The thickness of the two foam materials applied in our experiments is approximately two times smaller than the calculated values (Table 2) which ensures our assumption of a homogeneous zinc distribution within the porous electrode after the first charging process.

3.2. *Battery tests*

The battery tests described in this section were focused on the high specific area foam material with 45 pores per inch (MN045).

The polarization curve obtained with a battery containing one cell is represented in Fig. 4. This measurement was performed after the first charge and for a 100% charged cell. The values of cell voltage for each particular current density were measured after waiting periods of 30 s. The peak power of this cell is 13 W($1300\ W\ m^{-2}$) and was obtained at a current density of $2000\ A\ m^{-2}$. The excellent conductivity provided by homogeneously distributed zinc in the foam electrode and its highly porous structure (porosity of 0.8 approximately) are responsible for the high current density and the high peak power of the battery.

The power curves for bipolar stacks containing one to seven cells are plotted in Fig. 5. Due to the absence of shunt currents and the use of bifunctional electrodes with very similar electrochemical behaviour, the experimentally measured power of the batteries was very close to the expected value ($P_{\text{bipolar stack}} = N \times P_{\text{one cell}}$). For the bipolar stack with seven cells a peak power of 90 W was demonstrated. The polarization curve measured for the bipolar stack containing seven cells shows a battery voltage decay induced by the slow kinetics at the bifunctional oxygen electrode in the lower current range (0–$50\ mA\ cm^{-2}$). At current densities higher than $200\ mA\ cm^{-2}$ this voltage decay can be attributed to oxygen diffusion hindrance in the gas diffusion electrode.

Figure 6 demonstrates the availability of high discharge rates from the bipolar stack. The deep discharge experiment was performed with one cell and with the stack of seven cells at a current density of $1000\ A\ m^{-2}$. The power output was constant at ~ 9 W for one cell and ~ 63 W for the stack until 60% of the nominal capacity (8 A h) of the battery was discharged. The electrolyte temperature increased from 25 to 42.5 °C during the discharge experiment.

The cycle life performance was studied for a single cell. Figure 7 presents the charge and discharge potential against time plots obtained during the first cycle, the 14th cycle and during the first cycle after regeneration of the zinc-foam electrode. For the first cycle, the voltages during charge and discharge were 2.1 and 1.1 V, respectively. After 14 cycles the overvoltages increased for both reactions by about 100 mV. The higher polarization of the cell developing with increasing cycle numbers is due to an increase in polarization of the zinc-foam electrode. Visual observation showed a dense, compact zinc

Table 2. Data for the experimental conditions at the first charging process of the two foam electrodes (MN020 and MN045) and calculated maximum thickness of the foam which still guarantees a homogeneous current distribution at the limiting diffusion current

Cu foam electrodes	*Data for the experimental conditions*					*Maximum foam thickness (Equation 1)*
	$10^3 \times v_{el}$ /m s^{-1}	*Re*	*Sh*	$10^6 \times k_a$ /m s^{-1}	$\eta_2 - \eta_1$ /V	h_{max} /mm
MN020 ($h = 5$ mm)	12.6	30.7	78.5	5.2	0.2	7
MN045 ($h = 2$ mm)	31.6	31.9	47.8	7.7	0.2	4

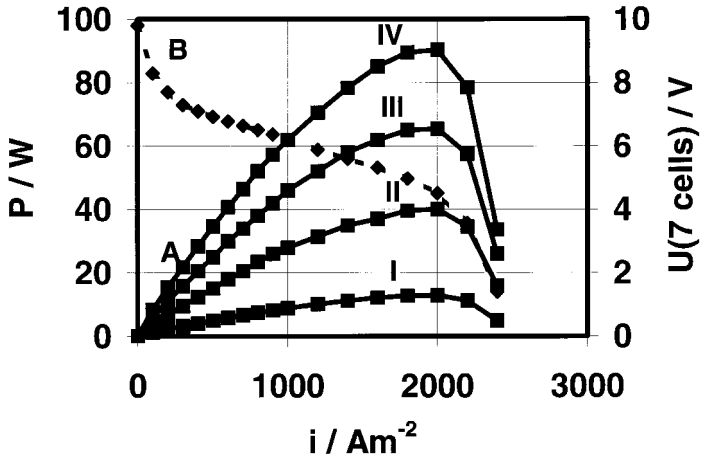

Fig. 5. Power curves (A) for bipolar stacks containing 1, 3, 5 and 7 cells (I–IV) and a plot of voltage against current density for the bipolar stack containing seven cells (B).

area at the bottom of the zinc-foam electrode. After regeneration of the three-dimensional electrode, the voltages were approximately 2.1 V for the charging and 1.1 V for the discharging process. The regeneration of the zinc-foam electrode (same conditions as for the first charging process) leads to a homogeneous zinc distribution within the electrode, and the battery could be cycled again with the same performance data as demonstrated for the first 14 cycles.

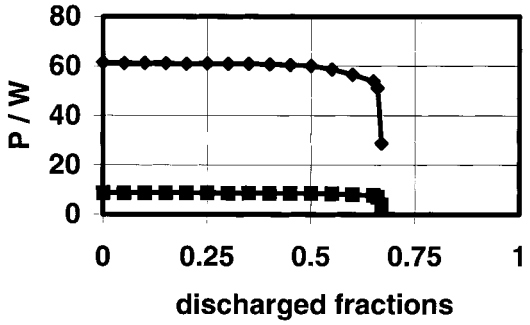

Fig. 6. Zinc/oxygen power and available capacity measured for a (■) single cell and for the (◆) bipolar stack with seven cells at a discharge current density of 1000 A m^{-2}.

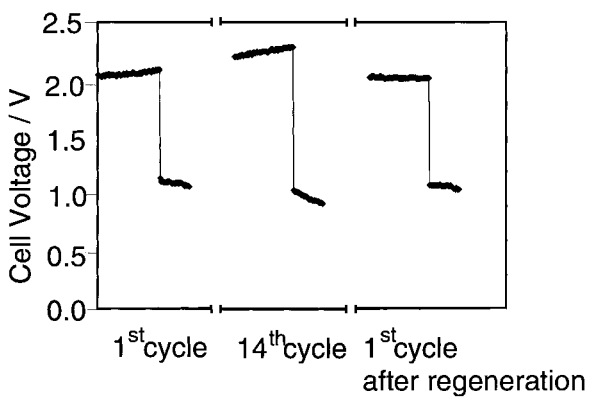

Fig. 7. Charge and discharge voltages during the first cycle, the 14th cycle and after regeneration of the foam electrode. Charge and discharge current densities are 100 and 200 A m^{-2}, respectively.

4. Conclusions

The combination of metallic foam as the support material for the zinc deposit in the Zn electrode with $La_{0.6}Ca_{0.4}CoO_3$-catalysed bifunctional oxygen electrodes results in a rechargeable zinc/oxygen battery showing peak power densities for a single cell of 130 mW cm^{-2} at 0.65 V. With a battery stack containing seven cells (100 cm^2) a peak power of 90 W was demonstrated. Approximately 60% of the nominal capacity (8 A h) could be discharged at a constant stack power of ~60 W.

Redistribution and dissolution of the zinc induced by natural convection resulted in a limited cycle life. However, a great advantage of the highly porous zinc electrode is its accessibility to electrolyte flow. At periodic service intervals the formation of new, well distributed zinc on the foam is possible by providing flowing highly alkaline electrolyte.

Acknowledgements

The authors acknowledge the financial support of this work provided by the Swiss Federal Office of Energy. We also thank Mrs G. Masanz for excellent technical support.

References

[1] L. Swette and N. Kackley, *J. Power Sources* **29** (1990) 423.
[2] T. C. Adler, F. R. McLarnon and E. J. Cairns, *J. Electrochem. Soc.* **140** (1993) 289.
[3] S. Müller, F. Holzer, O. Haas, C. Schlatter and Ch. Comninellis, *Chimia* **49** (1995) 27.
[4] *Idem*, Proceedings of the symposium on 'Rechargeable Zinc Batteries' commemorating the 100th birthday of A. N. Frumkin, 1995, *Electrochem. Soc. Proc.* **95–14** (1996) 135.
[5] A. Montillet, J. Comiti and J. Legrand, *J. Appl. Electrochem.* **24** (1994) 384.
[6] J. Newman and W. Tiedemann, *Adv. Electrochem. & Electrochem. Engng* **11** (1978) 353.
[7] G. L. Wierschem and W. H. Tiedemann, ECS Meeting, Hollywood, Fl (Oct. 1980), Abstract 102.
[8] Ch. Comninellis, *in* 'Electrochemical Engineering and Energy' (edited by F. Lapicque, A. Storck and A. A. Wragg), Plenum Press New York (1994).

[9] M. Rota, Ch. Comninellis, S. Müller, F. Holzer and O. Haas, *J. Appl. Electrochem.* **25** (1995) 114.
[10] J. F. Cooper, D. Fleming, L. Keene, A. Maimoni, K. Peterman and R. Koopman, 29th Intersociety Energy Conversion Engineering Conference, Monterey, CA 7–12 Aug. (1994).
[11] G. Kreysa, *Electrochimica Acta* **23** (1978) 1351.
[12] C. J. Brown, D. Pletcher, F.C. Walsh, J.K. Hammond and D. Robinson, *J. Appl. Electrochem.* **23** (1993) 38.
[13] A. Montillet, J. Comiti and J. Legrand, *ibid.* **24** (1994) 484.